Journal of Manufacturing Processes 100 (2023) 27–33

Contents lists available at ScienceDirect

Journal of Manufacturing Processes

journal homepage: www.elsevier.com/locate/manpro

Cold spray direct writing of flexible electrodes for enhanced performance triboelectric nanogenerators

Semih Akin [a,*], Young Won Kim [a], Shujia Xu [b], Chandra Nath [a,c], Wenzhuo Wu [b], Martin Byung-Guk Jun [a,c,d,**]

[a] School of Mechanical Engineering, Purdue University, West Lafayette, IN 47907, USA
[b] School of Industrial Engineering, Purdue University, West Lafayette, IN 47907, USA
[c] Maijker Corp., West Lafayette, IN 47906, USA
[d] Indiana Manufacturing Competitiveness Center (In-Mac), West Lafayette, IN 47907, USA

ARTICLE INFO

Keywords:
Additive manufacturing
Cold spray
Triboelectric nanogenerator (TENG)
Energy harvesting
Flexible polymer
Electrode
Polymer metallization

ABSTRACT

Triboelectric nanogenerator (TENG) is an emerging energy harvesting device to effectively harness various mechanical energy sources. In TENG technology, polymers are of particular interest as tribo-negative materials owing to their unique properties (*e.g.,* charge storage capability, impact resistance, flexibility, low cost, recyclability, *etc.*). Despite significant advances, one major challenge for TENG is to develop high-performance back electrodes that are conformably attached to the tribo-negative polymer substrates to fully exploit the potential of TENG in energy harvesting. To this end, the present study is aimed to employing direct "cold spray" particle deposition as just one-step fabrication method for high-performance electrodes on flexible polymers. In this regard, Tin (Sn) particles are directly written on the polymer (PET) surface by cold spraying to achieve conformal electrodes with high-adhesive strength and stable electrical conductivity. The resulting electrodes are thoroughly characterized in terms of microstructure, adhesion strength, and electrical performance. Arc-shaped TENG devices with both traditional aluminum (control) and cold-sprayed Sn electrodes are fabricated, followed by evaluating the TENGs' performance. Owing to the strong adhesion and micro-roughness (*i.e.*, $R_a = 4.865$ μm) of the Sn electrodes, electricity generation performance was found to be improved by ≈2.4 folds as compared to the control TENG. The TENG with Sn electrode can generate an open-circuit output voltage of up to 243 V with a maximum output power of 130 mW/m^2, thereby indicating the promising potential of the cold spray technique in TENG technology.

1. Introduction

Energy harvesting from the surrounding environment is of high importance for the sustainable development of society as it enables decreasing the consumption of environmentally-hazardous fossil fuels. In particular, the synergistic advance of small-scale electronics, the internet of things (IoT), and sensor fusion has led to a critical need for distributed energy sources, which can be provided by solar, wind, thermal, and water wave energy [1]. In this regard, since its invention in 2012 by Wang et al. [2], triboelectric nanogenerator (TENG) have gained tremendous attention to converting abundant surrounding energy sources into electrical energy [1]. Owing to its high efficiency, simplicity, low cost, and facile manufacturing, the practical viability of TENG has been demonstrated in various applications including, micro/nanoenergy sources [3,4], active sensing and self-powered sensors [5,6], and blue energy [7].

TENG, as a new source of energy harvesting device, mainly lies in the principle of contact electrification and electrostatic induction [8]. Basically, when two or more triboelectric materials having opposite polarities come into contact and then separated or slide against each other, electron transfer takes place between the materials, resulting in electrostatic charges on the surfaces of these triboelectric materials [2,8]. There are mainly four modes of TENG, which are (i) lateral sliding mode, (ii) vertical contact-separation mode, (iii) single-electron mode, and (iv) free-standing mode [1,9]. In lateral sliding type TENG, rotating and freestanding designs are widely used, whereas, in vertical contact-separation and single electrode modes, pressure and vibrations are

* Corresponding author.
** Corresponding author at: School of Mechanical Engineering, Purdue University, West Lafayette, IN 47907, USA.
E-mail addresses: sakin@purdue.edu (S. Akin), mbgjun@purdue.edu (M.B.-G. Jun).

https://doi.org/10.1016/j.jmapro.2023.05.015
Received 25 April 2023; Accepted 2 May 2023
Available online 10 May 2023

Nomenclature

Al	Aluminum
CS	Cold spray
PET	Polyethylene terephthalate
PI	Polyimide
Sn	Tin
TENG	Triboelectric nanogenerator

generally converted into electricity [10]. Although the lateral sliding mode shows higher output performance due to strong friction between the materials, it also has significant limitations, such as material choice, high manufacturing cost, complexity, and lack of durability [11]. Conversely, the vertical-contact mode TENG is a simple structure and it is widely used in various practical applications in mechanical dynamics systems [12].

In the TENG technology, the appropriate selection of negative and positive friction layers is vital to achieving desired output performance [13]. In this regard, many studies have focused on the selection of polymeric materials for high-performance TENG [14,15]. In addition to positive and negative friction layers, back electrode is also crucial to effectively trap and collect the charge for enhanced triboelectric output [16,17]. However, in TENG device design, less attention has been paid to the role of electrodes for effective charge collection [17] due to the manufacturing limitations. Considering the back electrode serves as a charge-collecting layer, the design and fabrication of electrodes on polymer surfaces are equally important for the mass production of high-performance TENG. The main electrode materials in TENG include gold (Au), copper (Cu), aluminum (Al), indium tin oxide (ITO), graphene, carbon, *etc.* [16,17]. These materials, however, have significant limitations, including, high-cost, low abundance, manufacturing complexity, *etc.* [16]. An ideal back electrode for a high-performance TENG device should meet the following requirements at the same time: i) conformal contact with the triboelectric polymer substrate, ii) high interfacial adhesive strength, iii) stable elastic behavior, iv) stable conductivity, and v) high-durability under severe working environments. However, current manufacturing techniques of back electrodes, for example, sputter coating, screen printing, vacuum deposition, *etc.,* have limitations to satisfy the aforementioned requirements at the same time. As such, a non-traditional manufacturing approach is of critical need to produce high-performance electrodes for TENG.

Herein, the emerging cold spray (CS) technique, by which the micron-scale metal particles are deposited on the target surface at high velocities, could address the aforementioned manufacturing limitations of the TENG technology. Owing to its low-process temperature, high-adhesive strength, and high-deposition rate, micron-scale metal particles (*e.g.*, Cu, Sn, *etc.*) can be directly deposited on various polymer surfaces in a mask- and vacuum-free manner [18–20]. Moreover, CS enables oxidation-free, dense, and micro-rough metal surface deposition on polymers [18], which are highly demanded features for tribolayers and back electrodes in the field of TENG.

Most recently, for the first time, the authors' group has incorporated the CS particle deposition technique into the TENG technology to produce composite triboelectric positive and negative friction layers [6]. As a noteworthy result, CS composite coatings significantly enhanced (6 times) the TENG performance owing to the micro-rough surface morphology and strong adhesion strength of the resulting CS deposits. Despite the state-of-the-art results [6], the main focus was given to the negative and positive friction layers more than the back electrodes. Considering back electrode is equally important as tribolayers [17], the CS technique could be also applied to the fabrication of back electrodes to produce high-performance TENG.

To this end, in the present study, we employ the emerging CS particle deposition technique for direct one-step fabrication of high-strength and conformal electrodes on flexible polymer substrates for TENG applications. In this regard, Tin (Sn) particles are directly written on the flexible polymer surface (*i.e.*, PET-polyethylene terephthalate) by the CS technique to fabricate the back electrode on the negative triboelectric substrate (PET) in a conformably embedded manner. The resulting electrodes are then characterized in terms of microstructure, adhesion strength, and electrical performance. The vertical contact-separation mode arc-shaped TENG devices with both traditional aluminum (Al) and CS-based Sn electrodes are fabricated and evaluated for their electricity generation performance. The key and novel contribution of the present work is the development of high-performance flexible back electrodes for TENG technology through the emerging CS deposition technique.

2. Structure and fabrication of TENG

In the present study, the vertical contact-separation mode TENG was chosen owing to its simplicity with various driving methods (*e.g.*, bending, vibration, *etc.*), numerous material options, long-life stability, and potential for industrial applications [12,21]. Next, as shown in Fig. 1a, the arch-shaped TENGs comprising different electrodes (*i.e.*, Al and Sn) on the negative tribo-layer (PET) were designed and fabricated. The TENGs were fabricated based on the arch-type design due to its simple fabrication and well-acceptance [12]. We intentionally chose to fabricate electrodes on the negative friction layer since the charge density on the negative layer is of great importance for TENG [22]. In both TENGs, Al film (Reynolds, thickness = 12 μm) is used as the positive tribo-layer and the positive electrode. As for the negatively charged element, a flexible PET polymer sheet (McMaster-Carr, thickness = 250 μm) was chosen. For the electrode on the negative frictional layer, Al was selected for the control TENG while the Sn electrode was fabricated by cold spraying. As such, these two configurations shown in Fig. 1a can enable performance comparison of the different electrodes (*i.e.*, Al and Sn), and also the feasibility test of the CS deposition in TENG technology.

As seen in Figs.1a-b, polyimide (PI) film with a thickness of 1.25 mm was used as the substrate to construct the vertical contact-separation mode arc-shaped TENGs. The PI film was cut into a rectangular shape having the dimensions of 63.5 mm × 200 mm, which was followed by folding of the as-cut PI film to build a self-elastic substrate with a certain gap (25 mm) between the positive and negative friction layers [6]. This arch-shaped PI substrate allows for the contact of the tribo-layers with each other when an input pressure is applied. When the pressure is released, the PI film turns back to the initial position due to its intrinsic elasticity, which allows a controllable contact and separation motion to test the performance of the TENG by hand tapping. This configuration ensures robust contact, alignment, and overlap between the friction layers.

The positive and negative parts were then assembled on the PI substrate by using foam mounting tape (see Fig. 1b). Lastly, the wires (Al tape) were attached to the positive and negative electrodes as the charge collector. A representative image of the TENG with the Sn electrode on the negative friction layer is shown in Fig. 1b. All the layers are in 25.4 mm wide and 25.4 mm long, thereby the contact area of the triboelectric effect is ≈ 645 mm^2.

Sn electrodes were directly deposited on the negative PET polymer sheet by employing a low-pressure CS machine (Rus Sonic Technology, Inc., Model: K205/407R) mounted on a programmable multi-axis robot arm (see Fig. 2a). In the CS process, as shown in Fig. 2b, micron-scale (5–50 μm) metal particles are accelerated to supersonic velocities (>350 m/s) by a high-pressure gas jet flowing through a converging-diverging nozzle [23–26]. When the high-speed particles impact the target surface, the particles' kinetic energy disperses onto the polymer surface, facilitating the high-strain rate metallurgical bonding of the particles, which further leads to a thick and well-consolidated metal

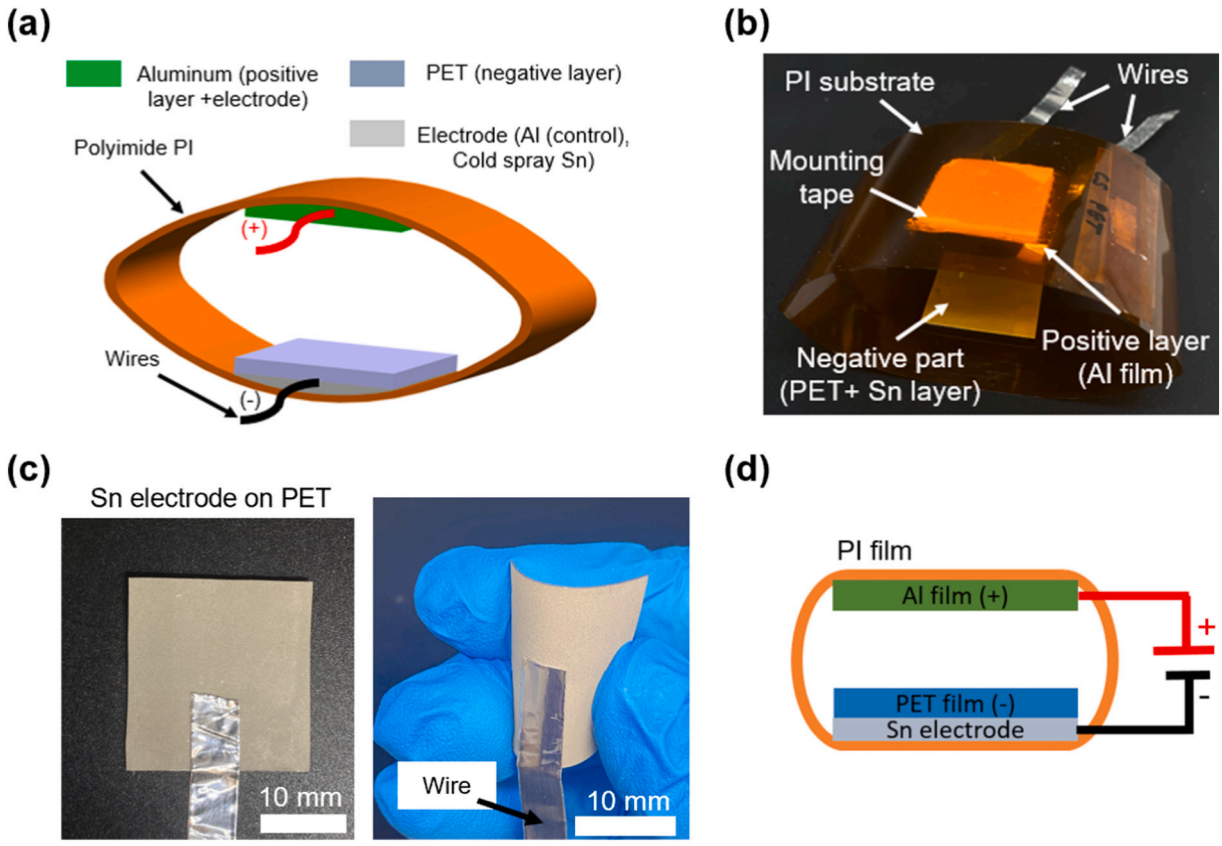

Fig. 1. Structure and fabrication process of the TENG: (a) Schematic illustration of typical arch-shaped TENG; (b) Image of the fabricated TENG with CS-based Sn electrode embedded on the negative tribo-layer, (c) Images of the flexible CS-based Sn electrodes; (d) cross-section schematic of the TENG with the Sn electrode.

coating on the target surface [27]. Owing to the low heat input of the CS process, the feedstock coating material maintains its phase with minimal or no oxidation, thereby having the potential for temperature-sensitive materials such as PET polymer [27,28]. Moreover, owing to the high-speed impingement of the particles onto the target surface, high-bond (adhesion) strength metal coating can be achieved by the CS process [29].

As for the coating material, micron-scale (10–45 μm) Sn particles (see the red box in Fig. 2b) were chosen due to its (i) high corrosion resistance; (ii) low melting temperature; (iii) high-electrical conductivity and stability [30]. In the CS experiments, a rectangular nozzle configuration (Fig. 2a, right panel) was used to process the large area coating due to a larger exit aperture of the rectangular nozzle as compared to typical axisymmetric cold spray nozzles [31]. Air was used as the propellant gas and the gas temperature was measured as 80 °C at the nozzle tip using an IR thermometer. The multi-axis robot arm (Kuka KR Agilus) was pre-programmed for precisely writing the Sn particles on the PET target. The CS operational parameters and robot arm kinematic parameters were adopted from the authors' previous work [32]. The nozzle dimensions and the process settings of the CS experiments are listed in Table 1.

3. Results and discussion

3.1. Characterization of the CS-written electrodes

The back electrode was fabricated by CS direct writing of Sn particles on the flexible negative layer (PET) using the operational conditions

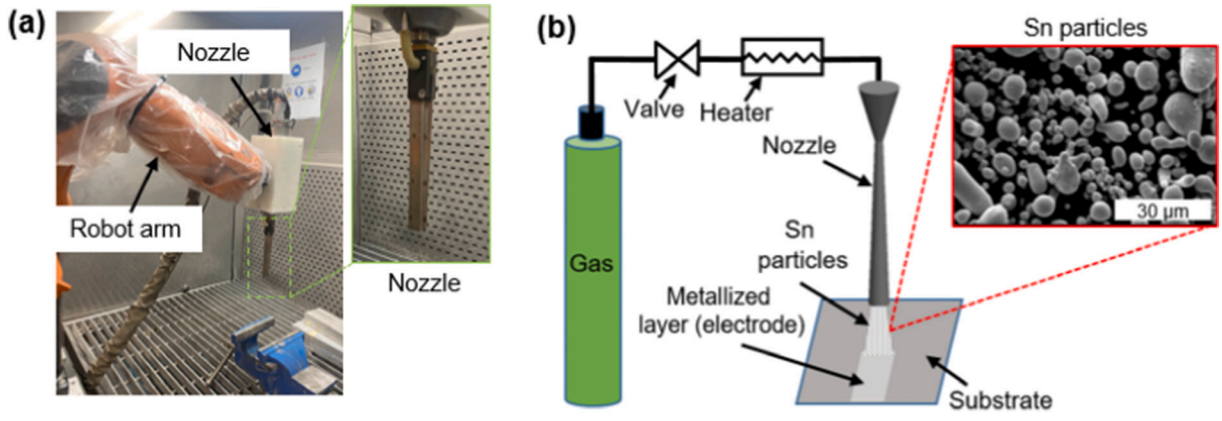

Fig. 2. (a) Images of the CS experimental setup; (b) the schematic of the CS direct writing process.

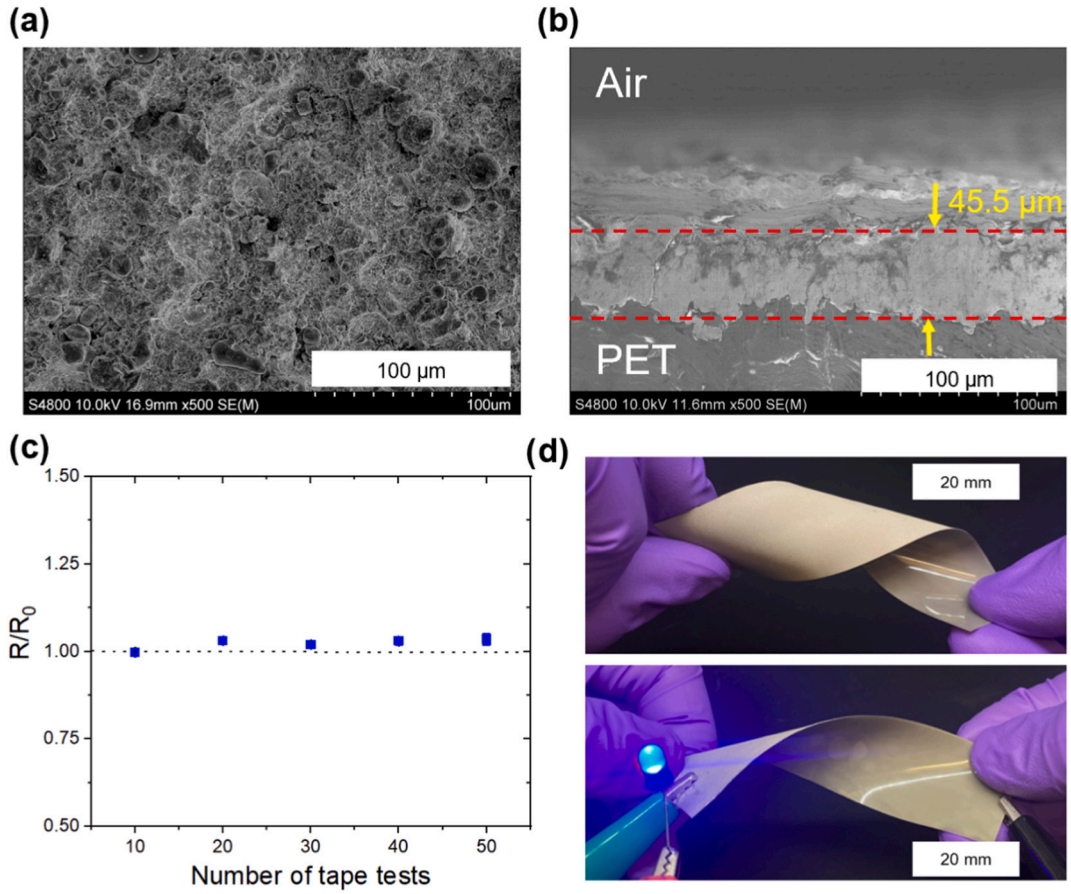

Fig. 3. Characterization of CS direct writing process: (a) microstructure of the CS Sn coating on the PET film; (b) Cross-section SEM image of the Sn coating; (c) Relative resistance (R/R_0) change of the electrodes under peeling tests; (d) Images of the Sn electrodes under twisting deformation.

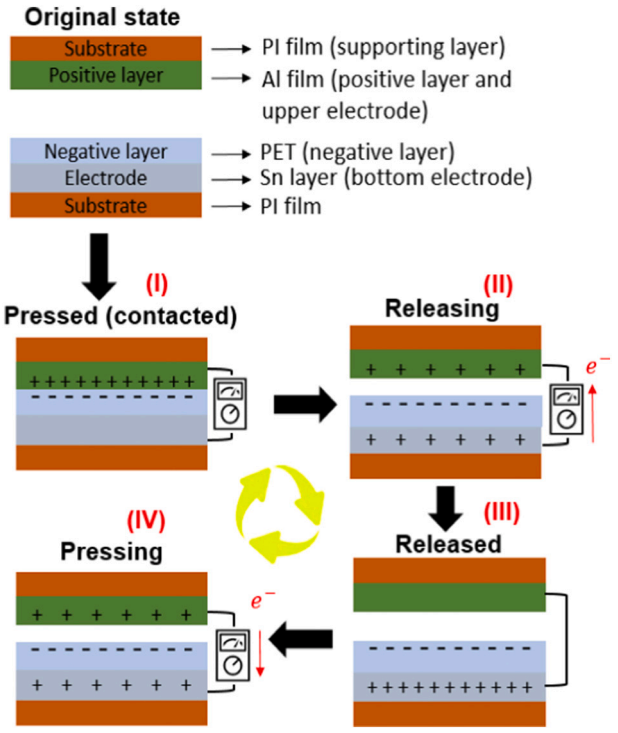

Fig. 4. Schematic of the working mechanism (charge transfer) of a vertical contact-separation mode TENG.

given in Table 1. Fig. 3a-b show the surface and cross-sectional microstructure of the resulting Sn electrode on the PET polymer. As seen in Fig. 3a, the well-consolidated metal (Sn) coating with negligible porosity was achieved. The Sn particles were metallurgically bonded on the target polymer surface, resulting in a relatively thick and uniform metal coating with a micro-rough (*i.e.*, R_a = 4.865 μm) surface morphology (see Fig. 3b). The average thickness of the coating was calculated at around 45.5 μm. The adhesion performance of the Sn electrodes was characterized by the Scotch tape (3 M) test method [33]. Numerous tape test (10–50 cycles) was applied to the surface of the electrodes by repeatedly attaching and detaching the tape from the as-CS Sn electrodes. Then the tape was peeled off from the electrode surface and visually inspected. Simultaneously, we recorded the relative resistance (R/R_0) after each test cycle, and the results are plotted in Fig. 3c. No significant alteration in the R/R_0 was noticed during the test (Fig. 3c), indicating a strong adhesion strength between the CS Sn coating and the PET substrate.

The electrical conductivity of the Sn electrodes was also calculated by using Eq. (1), where σ is the conductivity, L is the length, R is the resistance, and S is the cross-sectional area of the Sn electrode. For a test electrode with L = 0.025 m, the resistance was measured by the two-point probe method as R = 0.163 Ω by using a digital multimeter (Agilent/HP 34401A). The cross-sectional area, S, was then calculated as $S = 2.275 \times 10^{-7}$ m^2 (*i.e.*, width (≈5 mm) × thickness (45.5 μm)). Collectively, the electrical conductivity of the electrode was obtained as 6.742×10^5 $S.m^{-1}$, which is only one order less than the bulk conductivity of the Sn (*i.e.*, 9.17×10^6 $S.m^{-1}$), indicating excellent electrical conductivity. Besides, both adhesion strength and conductivity of the electrodes were evaluated under twisting/kinking deformation (>100 cycles with the twisting angle of 0°–180°). As seen in Fig. 3d, the

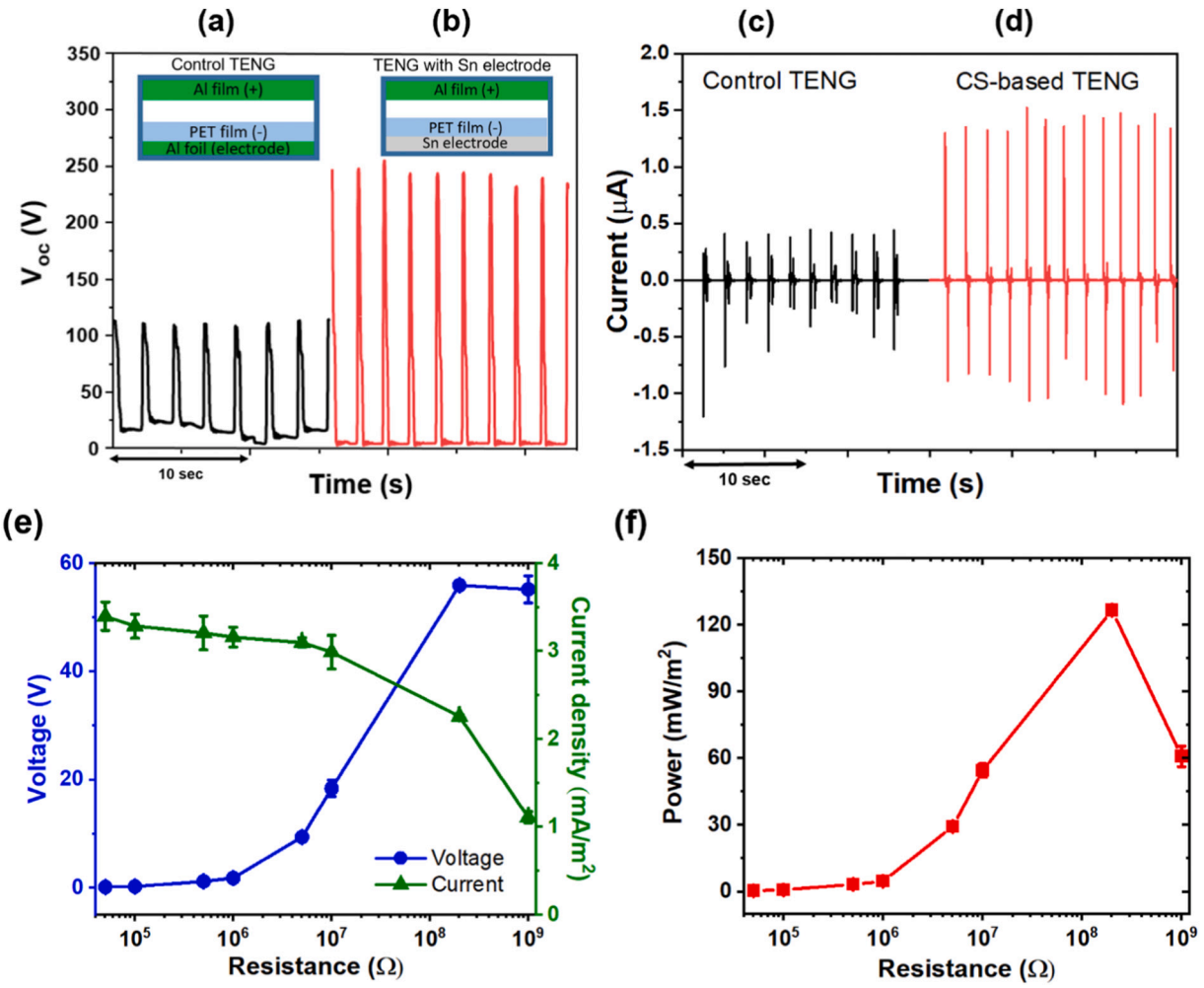

Fig. 5. Triboelectric output voltage of the TENGs using (a) Al foil as the electrode; (b) Sn as the electrode; Triboelectric output current for (c) control TENG with Al electrode; (d) CS-based TENG; (e) Output voltage and current density of the TENG with Sn electrode at various load resistance; (f) Maximum output power of the TENG with the Sn electrode at various load resistance.

Table 1
Nozzle dimensions and cold spray settings.

Procedure	Parameter	Setting	Unit
Nozzle dimensions	Inlet diameter	9	mm
	Convergent length	15	mm
	Throat diameter	4	mm
	Divergent length	140	mm
	Nozzle outlet dimensions	10.35 × 3	mm × mm
Cold spray experiments	Driving gas	Air	–
	Driving gas pressure	0.7	MPa
	Driving gas temperature	80	°C
	Powder feed rate	12	g/min
	Nozzle transverse speed	75	mm/s
	Spray distance	10	mm
	Number of spray pass	1	–

fabricated Sn electrodes exhibited stable conductivity without any sign of crack formation and delamination under harsh deformation. This also confirms the reliability of the fabricated electrodes under repeated loading. Taken together, the results reveal that the CS direct writing ensures the Sn electrodes on the flexible polymer surface with excellent adhesion strength, electrical conductivity, and stability without compromising intrinsic polymer and electrode properties.

$$\sigma = \frac{L}{RS} \quad (1)$$

3.2. Working mechanism of the TENG

Following the CS direct writing of Sn, the TENGs were fabricated for energy harvesting characterizations. Fig. 4 illustrates the working mechanism of a typical vertical contact-separation mode TENG, where the PI is served as a supporting structure, Al film is the positive friction layer and the positive electrode, and PET is the negative layer having Sn and Al (control) back electrodes. Basically, the working mechanism of a TENG relies on the coupling of triboelectrification and electrostatic induction [34].

Principally, as shown in Fig. 4, a complete working cycle of a contact-separation mode TENG involves four processes: contacting (pressing), contacted (pressed), separating (releasing), and separated (released) [12,35]. To elaborate, at the original stage where there is no contact, charge transfer does not occur due to the electrostatic equilibrium between the materials. When an input pressure is applied to the TENG in the vertical direction, the positive and negative layers contact together, leading to charge polarization. When the pressure is released, the friction layers begin separating from each other due to the intrinsic elastic force of the PI substrate.

As the friction layers separate from each other, the potential difference between the positive layer (Al) and the negative layer (PET) drives electrons from the lower electrode (Sn) to the upper electrode (Al) through an external circuit. When the positive and negative layers are fully separated, no charge transfer forms due to the screening of the

charges on the negative layer by the induced charges on the electrodes [35]. When the layers are pressed again, the electrostatic equilibrium is broken, resulting in an opposite charge transfer from the positive electrode (Al) to the negative electrode (Sn). As such, the repeated contact/separation between the positive and negative friction layers under an external mechanical load induces cyclic charge transfer in electrodes, leading to the conversion of mechanical energy into electrical energy.

3.3. Performance evaluation of the TENGs

To explore the performance of the fabricated devices, an external load should be applied to TENG. In this regard, hand-tapping cycles (*i.e.*, 1 hand taping per 2 s) were applied to both TENGs for 16 s. A programmable electrometer (Keithley 6514) was used to measure the open-circuit voltage, short-circuit current, and current and power densities. Fig. 5a-b show the open-circuit voltage generation of the TENGs having the negative electrodes made of Al film and CS written Sn, respectively. The TENG with the Sn electrode generated significantly better performance (≈2.4 times higher) than that of the control TENG with a conventional negative Al electrode. The CS-based TENG generated a maximum open-circuit voltage of 243 V while the control TENG produced an average voltage of ≈100 V. Moreover, Fig. 5c-d present the current measurement results of the TENGs as a function of time. As seen in Fig. 5c-d, the TENG with Sn electrode showed better performance than the control TENG in terms of the current movement. The enhanced performance of the CS-based TENG is attributed to: i) the synergistic tribo-activity between the negative PET layer and the as-CS Sn electrode due to the resultant rough surface, which improved the flow of charge [36] and ii) the strong adhesion strength and conformal contact of the Sn electrode with the substrate for better charge trapping. Surface roughness and adhesive strength (*i.e.*, intimate contact) of tribo-surfaces are responsible for the capacitance, dielectric constant, and dipole moment of the friction layers, leading to additional triboelectric charges [36,37].

Triboelectric voltage output and power generation were also characterized for the CS-based TENG at various external load resistance (from 50 kΩ to 1 GΩ) as shown in Fig. 5e-f, respectively. The maximum voltage of 56 V was achieved at the load resistance of 200 MΩ. Further increase in resistance led to a voltage drop due to the external resistance. Also, the voltage difference at different resistance loads is attributed to the internal resistance of the device [6]. As for the current density in Fig. 5e, the maximum current density was obtained as 3.4 mA/m^2 where the load resistance is 50 kΩ. Again, larger resistance than a threshold (>50 kΩ) resulted in lower current density. Moreover, the power generation was also characterized at different external load resistors, and a maximum power of 130 mW/m^2 was achieved using the CS-based TENG (see Fig. 5f). Taken together, these proof-of-the concept results reveal that the CS-based back electrode effectively improved the TENG's performance owing to its improved surface roughness, adhesive strength, and conformal contact with the negative layer.

4. Conclusion

In this study, the cold spray (CS) particle deposition technique was employed for direct writing of flexible polymer electrodes for TENG technology for enhancing energy harvesting performance. The following results can be drawn from the present study:

- CS enabled to produce micro-rough (R_a = 4.865 μm) Sn electrodes with excellent electrical conductivity (6.742 × 10^5 S.m^{-1}) and adhesion strength, which significantly improved the TENG's performance
- The voltage generation performance of the CS-based TENG was found to be 2.4 fold higher than the control TENG with the traditional Al electrode.
- A maximum output open-circuit voltage of 243 V and current density of 3.4 mA/cm^2 were achieved by the CS-based TENG.
- The improved performance of the TENG is attributed to strong and conformal contact of the CS written Sn electrode with the negative PET layer, which increased the charge trapping and electron transfer.
- The results revealed that the CS technique can be successfully used as just one-step fabrication method of high-performance flexible electrodes for TENG, thereby having the potential to synergistically advance the TENG technology for many practical applications, especially in distributed micro/nano energy sources.
- Moreover, owing to its multi-axis processing capability with robot framework, the CS-based electrode fabrication approach in this study can be also applied to the large-scale production of complex-shaped TENG devices.

Declaration of competing interest

The authors declare that they have no known competing financial interests or personal relationships that could have appeared to influence the work reported in this paper.

References

[1] Wu C, Wang AC, Ding W, Guo H, Wang ZL. Triboelectric nanogenerator: a foundation of the energy for the new era. Adv Energy Mater 2019;9:1802906. https://doi.org/10.1002/aenm.201802906.
[2] Fan FR, Tian ZQ, Lin Wang Z. Flexible triboelectric generator. Nano Energy 2012;1:328–34. https://doi.org/10.1016/J.NANOEN.2012.01.004.
[3] Yang W, Chen J, Zhu G, Yang J, Bai P, Su Y, et al. Harvesting energy from the natural vibration of human walking. ACS Nano 2013;7:11317–24. https://doi.org/10.1021/NN405175Z/SUPPL_FILE/NN405175Z_SI_002.AVI.
[4] Lee JG, Kim DY, Lee JH, Kim MW, An S, Jo HS, et al. Scalable binder-free supersonic cold spraying of nanotextured cupric oxide (CuO) films as efficient photocathodes. ACS Appl Mater Interfaces 2016;8:15406–14. https://doi.org/10.1021/acsami.6b03968.
[5] Wang Y, Yang Y, Wang ZL. Triboelectric nanogenerators as flexible power sources. Npj Flex Electron 2017;1:1–10. https://doi.org/10.1038/s41528-017-0007-8. 2017 11.
[6] Kim YW, Akin S, Yun H, Xu S, Wu W, Byung M, et al. Enhanced performance of triboelectric nanogenerators and sensors via cold spray particle deposition. ACS Appl Mater Interfaces 2022. https://doi.org/10.1021/ACSAMI.2C09367.
[7] Wang ZL. Catch wave power in floating nets. Nat 2017;542:159–60. https://doi.org/10.1038/542159a. 2017 5427640.
[8] Lin Wang Z, Wang ZL. Triboelectric nanogenerator (TENG)—sparking an energy and sensor revolution. Adv Energy Mater 2020;10:2000137. https://doi.org/10.1002/AENM.202000137.
[9] Zhang H, Han M, Zhang X. Structures of triboelectric nanogenerators. Flex Stretchable Triboelectric Nanogenerator Devices Towar Self-Powered Syst 2019:19–40. https://doi.org/10.1002/9783527820153.CH2.
[10] Wang ZL, Lin L, Chen J, Niu S, Zi Y. In: Triboelectric nanogenerator: lateral sliding mode; 2016. p. 49–90. https://doi.org/10.1007/978-3-319-40039-6_3.
[11] Zhou L, Liu D, Zhao Z, Li S, Liu Y, Liu L, et al. Simultaneously enhancing power density and durability of sliding-mode triboelectric nanogenerator via Interface liquid lubrication. Adv Energy Mater 2020;10:2002920. https://doi.org/10.1002/AENM.202002920.
[12] Kim YW, Lee HB, Yoon J, Park SH. 3D customized triboelectric nanogenerator with high performance achieved via charge-trapping effect and strain-mismatching friction. Nano Energy 2022:95. https://doi.org/10.1016/j.nanoen.2022.107051.
[13] Chen A, Zhang C, Zhu G, Wang ZL. Polymer materials for high-performance triboelectric nanogenerators. Adv Sci 2020:7. https://doi.org/10.1002/advs.202000186.
[14] Godwinraj D, George SC. Recent advancement in TENG polymer structures and energy efficient charge control circuits. Adv Ind Eng Polym Res 2021;4:1–8. https://doi.org/10.1016/J.AIEPR.2020.12.003.
[15] Aazem I, Dhanu A, Mathew T, Radhakrishnan S, Vijoy KV, John H, et al. Electrode materials for stretchable triboelectric nanogenerator in wearable electronics. 2022. https://doi.org/10.1039/d2ra01088g.
[16] Šutka A, Timusk M, Metsik J, Ruža J, Knite M, Mäeorg U. PEDOT electrodes for triboelectric generator devices. Org Electron 2017;51:446–51. https://doi.org/10.1016/J.ORGEL.2017.09.052.
[17] Zhao P, Bhattacharya G, Fishlock SJ, Guy JGM, Kumar A, Tsonos C, et al. Replacing the metal electrodes in triboelectric nanogenerators: high-performance laser-induced graphene electrodes. Nano Energy 2020:75. https://doi.org/10.1016/J.NANOEN.2020.104958.
[18] Melentiev R, Yu N, Lubineau G. Polymer metallization via cold spray additive manufacturing: a review of process control, coating qualities, and prospective applications. Addit Manuf 2021;48:102459. https://doi.org/10.1016/j.addma.2021.102459.
[19] Tsai J-T, Akin S, Zhou F, Bahr DF, Jun MB-G. Establishing a cold spray particle deposition window on polymer substrate. J Therm Spray Technol 2021:1–12. https://doi.org/10.1007/s11666-021-01179-x.

[20] Akin S, Wu P, Tsai J-T, Nath C, Chen J, Jun MB-G. A study on droplets dispersion and deposition characteristics under supersonic spray flow for nanomaterial coating applications. Surf Coat Technol 2021;426:127788. https://doi.org/10.1016/j.surfcoat.2021.127788.
[21] Lee Y, Kim W, Bhatia D, Hwang HJ, Lee S, Choi D. Cam-based sustainable triboelectric nanogenerators with a resolution-free 3D-printed system. Nano Energy 2017;38:326–34. https://doi.org/10.1016/J.NANOEN.2017.06.015.
[22] Lin S, Wang ZL. Scanning triboelectric nanogenerator as a nanoscale probe for measuring local surface charge density on a dielectric film. Appl Phys Lett 2021; 118:193901. https://doi.org/10.1063/5.0051522.
[23] Papyrin A, Kosarev V, Klinkov S, Alkhimov A, Fomin VM. Cold spray technology. Elsevier Ltd; 2007. https://doi.org/10.1016/B978-0-08-045155-8.X5000-5. 2017 11.
[24] Villafuerte J. Modern cold spray: materials, process, and applications. Springer International Publishing; 2015. https://doi.org/10.1007/978-3-319-16772-5.
[25] Tsai J-T, Akin S, Zhou F, Park MS, Bahr DF, Jun MB-G. Electrically conductive metallized polymers by cold spray and co-electroless deposition. ASME Open J Eng 2022:1. https://doi.org/10.1115/1.4053781.
[26] Akin S, Tsai J-T, Park MS, Jeong YH, Jun M. Fabrication of electrically conductive patterns on ABS polymer using low-pressure cold spray and electroless plating. J Micro Nano-Manuf 2021:8. https://doi.org/10.1115/1.4049578.
[27] Della Gatta R, Perna AS, Viscusi A, Pasquino G, Astarita A. Cold spray deposition of metallic coatings on polymers: a review. J Mater Sci 2022;57:27–57. https://doi.org/10.1007/s10853-021-06561-2.
[28] Akin S, Jo S, Jun MBG. A cold spray-based novel manufacturing route for flexible electronics. J Manuf Process 2023;86:98–108. https://doi.org/10.1016/j.jmapro.2022.12.035.
[29] Zhang D, Shipway PH, McCartney DG. Cold gas dynamic spraying of aluminum: the role of substrate characteristics in deposit formation. J Therm Spray Technol 2005;14:109–16. https://doi.org/10.1361/10599630522666.
[30] Liberati AC, Che H, Fallah P, Vo P, Yue S. Pull-off testing and electrical conductivity of sn-based metal powder mixtures cold sprayed on carbon fiber-reinforced polymers. J Therm Spray Technol 2022:1–21. https://doi.org/10.1007/s11666-022-01405-0.
[31] Gabor T, Akin S, Tsai J-T, Jo S, Al-Najjar F, Jun MB-G. Numerical studies on cold spray particle deposition using a rectangular nozzle. In: Addit manuf biomanufacturing; life cycle eng manuf equip autom nano/micro/meso manuf. Vol 1; 2022. https://doi.org/10.1115/MSEC2022-85673.
[32] Akin S, Lee S, Jo S, Ruzgar DG, Subramaniam K, Tsai J-T, et al. Cold spray-based rapid and scalable production of printed flexible electronics. Addit Manuf 2022;60: 103244. https://doi.org/10.1016/J.ADDMA.2022.103244.
[33] Modesto-López LB, Miettinen M, Torvela T, Lähde A, Jokiniemi J. Direct deposition of graphene nanomaterial films on polymer-coated glass by ultrasonic spraying. Thin Solid Films 2015;578:45–52. https://doi.org/10.1016/j.tsf.2015.01.073.
[34] Karan SK, Maiti S, Lee JH, Mishra YK, Khatua BB, Kim JK. Recent advances in self-powered tribo-/piezoelectric energy harvesters: all-in-one package for future smart technologies. Adv Funct Mater 2020;30:2004446. https://doi.org/10.1002/ADFM.202004446.
[35] Xiao Y, Lv X, Yang L, Niu M, Liu J. A high-performance flexible triboelectric nanogenerator based on double-sided patterned TiN/PDMS composite film for human energy harvesting. Energy Technol 2021:9. https://doi.org/10.1002/ENTE.202100665.
[36] Fan B, Liu G, Fu X, Wang Z, Zhang Z, Zhang C. Composite film with hollow hierarchical silica/perfluoropolyether filler and surface etching for performance enhanced triboelectric nanogenerators. Chem Eng J 2022;446:137263. https://doi.org/10.1016/J.CEJ.2022.137263.
[37] Mariello M, Scarpa E, Algieri L, Guido F, Mastronardi VM, Qualtieri A. Novel flexible triboelectric nanogenerator based on metallized porous PDMS and Parylene C. Energies 2020;13:1625. https://doi.org/10.3390/EN13071625. 2020, Vol 13, Page 1625.